RESEARCH PROGRESS IN MECHANICAL AND MANUFACTURING ENGINEERING
e-ISSN: 2773-4765

RPMME

Vol. 6 No. 2 (2025) 18-26
https://publisher.uthm.edu.my/periodicals/index.php/rpmme

Effect of Composition on the Properties of Silica Foam Produced by Slurry Method

Puteri Nur Syafiqah Nor Zaidin[1], Sufizar Ahmad[1*]

[1] *Faculty of Mechanical and Manufacturing Engineering, Universiti Tun Hussein Onn Malaysia, 86400 Parit Raja, Batu Pahat, Johor, MALAYSIA*

*Corresponding Author: sufizar@uthm.edu.my
DOI: https://doi.org/10.30880/rpmme.2025.06.02.003

Article Info

Received: 20 June 2025
Accepted: 30 October 2025
Available online: 10 Disember 2025

Keywords

Density, Carboxymethyl cellulose, Compressive strength, Polyethylene glycol, Porosity, Silica, Slurry foam

Abstract

This study explores the fabrication of silica foam derived from rice husk-based silica for potential use in water filtration systems. Silica served as the primary material, while polyethylene glycol (PEG) and carboxymethyl cellulose (CMC) were employed as binders in the slurry formulation. The investigation focused on the influence of different silica compositions, specifically 45 wt.%, 50 wt.%, and 55 wt.% at a constant sintering temperature of 1200°C. The resulting foams were characterized through morphological analysis using Scanning Electron Microscopy (SEM), density and porosity measurements following ASTM C20 standards, and compressive strength testing in accordance with ASTM C773-88. Pore sizes ranged from 237.12 µm to 452.08 µm. Foam analysis revealed an inverse relationship between density and porosity. The optimal density (0.5591 g/cm^3) was recorded at 50 wt%, while maximum porosity (69.61%) occurred at 45 wt.%. Compressive strength peaked at 55 wt.% (0.162 N/mm^2), indicating sufficient mechanical integrity. The findings underscore the significance of slurry composition, curing, and application methods in achieving optimal structural and mechanical properties. Overall, the replication method proved effective in producing silica foams with promising characteristics for sustainable and efficient water filtration applications.

1. Introduction

Ceramic foams are lightweight, porous materials known for their excellent thermal stability, mechanical strength, and chemical resistance, making them ideal for applications such as thermal insulation, filtration, and catalyst support. Among various ceramic materials, silica (SiO_2) stands out due to its natural abundance, high melting point, and durability [1]. Silica foams, in particular, offer a favorable combination of low density and high porosity, enhancing their performance in insulation and filtration systems.

The slurry method is a widely adopted fabrication technique for ceramic foams, involving the use of ceramic powders, binders, and additives to form a porous structure upon sintering [2]. The final properties of the foam are significantly influenced by the slurry composition and sintering temperature. While appropriate thermal treatment enhances densification and mechanical strength, excessive sintering temperatures may lead to undesirable crystallization and reduced performance. This study investigates the effects of varying silica content and sintering temperatures on the structural and mechanical properties of silica foams produced via the slurry method. By analyzing parameters such as microstructure, density, porosity, and compressive strength, the research aims to optimize the fabrication process and contribute to the development of high-performance, sustainable silica-based materials for industrial applications.

Research Progress in Mechanical and Manufacturing Engineering Vol. 6 No. 2 (2025) p.18-26

2. Methodology

2.1 Sample Preparation

For this study, silica foam samples were prepared using the slurry method with polyurethane (PU) foam as a template. The slurry consisted of silica as the primary material, along with polyethylene glycol (PEG), carboxymethyl cellulose (CMC), and distilled water. A total of 27 cylindrical samples were prepared for three types of testing. The preparation involved three key parameters, three types of testing, and three repetitions for each condition as shown in Table 1. Each sample measured approximately 13 mm in diameter and 26 mm in height. Fig. 1 shows the schematic presentation of the foam replica method.

Table 1 *Sampling data*

Silica (wt. %)	Sample
45	A1-1-45, B1-2-45, C1-3-45 A2-1-45, B2-2-45, C2-3-45 A3-1-45, B3-2-45, C3-3-45
50	A1-1-50, B1-2-50, C1-3-50 A2-1-50, B2-2-50, C2-3-50 A3-1-50, B3-2-50, C3-3-50
55	A1-1-55, B1-2-55, C1-3-55 A2-1-55, B2-2-55, C2-3-55 A3-1-55, B3-2-55, C3-3-55

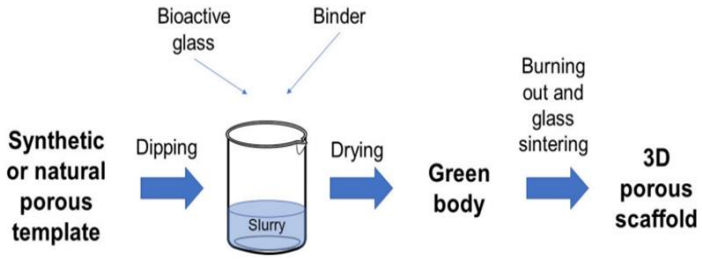

Fig. 1 *Schematic representation of the foam replica method*

2.2 Microstructure Observation

Scanning Electron Microscopy (SEM) was used to examine the microstructure of the silica foam samples at high resolution. This technique allowed for detailed observation of pore size, strut structure, and changes in porosity after sintering. Since silica is non-conductive, samples were coated with a thin layer of gold to prevent charge buildup and ensure image clarity. Each sample was mounted using carbon tape and scanned using a SU150 VP-SEM. The SEM images provided critical insights into the effects of sintering on the foam's structure, helping to identify optimal processing conditions.

2.3 Density and Porosity Test

The density and porosity of the sintered silica foam samples were determined using the immersion method based on Archimedes' principle, following ASTM C20 standards. The procedure involved measuring the sample's dry weight (Wd), saturated weight (Ws), and submerged weight (Ww) using a Mettler Toledo Density Determination Kit. Samples were soaked in boiling distilled water for 5 hours, followed by an additional 22 hours of soaking at room temperature. These measurements were used to calculate bulk density and open porosity, providing insight into the foam's internal structure and sintering effectiveness. These values were used in equations 1 and 2 to calculate the density and porosity, providing insights into the sample's internal structure and the effectiveness of the sintering process.

$$\text{Density} = \frac{wd}{wd - ws} \quad (1)$$

$$\text{Porosity percentage} = \frac{ww - wd}{ww - ws} \times 100\% \quad (2)$$

2.4 Compressive Strength Test

The compressive strength of the sintered silica foam samples was evaluated using a Shimadzu Autograph AG-10kN universal testing machine, following ASTM C773-88 standards. Cylindrical samples were tested at a loading rate of 0.5 mm/min until failure. The maximum load at fracture was recorded and used to calculate compressive strength by dividing it by the sample's cross-sectional area. Three samples from each composition were tested, and the average value was reported to ensure accuracy and consistency. The test results were displayed on the computer, and the compression strength was calculated by dividing the maximum load by the cross-sectional area of the sample, as shown in equation 3.

$$S = \frac{P}{\frac{\pi d^2}{4}} \quad (3)$$

Where, S = Compression Strength
P = Maximum Force
d = Diameter of sample

3. Result and Discussion

3.1 Morphology Analysis of Silica Foam

The morphology of the silica foams was analyzed to examine pore connectivity and strut uniformity at different silica compositions. Fig. 2, 3 and 4 present the SEM micrographs of foams fabricated with 45 wt%, 50 wt%, and 55 wt% silica. The blue circles in the table represent open pores, while purple circles denote closed pores.

All samples C1-1-45, C1-2-45, and C1-3-45 were examined at 50x and 1000x magnification to analyze the pore morphology and strut microstructure of silica foam at 45 wt.% composition. Samples C1-1-45, C1-2-45, and C1-3-45 all exhibit a heterogeneous pore network composed of circular open and closed pores randomly distributed throughout the structure. This configuration facilitates efficient fluid permeability while maintaining structural rigidity—an ideal balance for filtration media [3]. C1-1-45 features moderately rough struts that increase the effective surface area for particle capture. C1-2-45 shows enhanced surface roughness and finer grain morphology, indicating high-quality sintering and improved filtration kinetics. C1-3-45 demonstrates consistent pore geometry with no visible defects, and its well-textured struts contribute to optimized contact surfaces, crucial for maximizing filtration efficiency. The observed pore morphology agrees with the foam replication theory, which suggests that increased binder uniformity enhances pore interconnectivity and wall integrity [4].

Sample	50x magnification	1000x magnification
C1-1-45	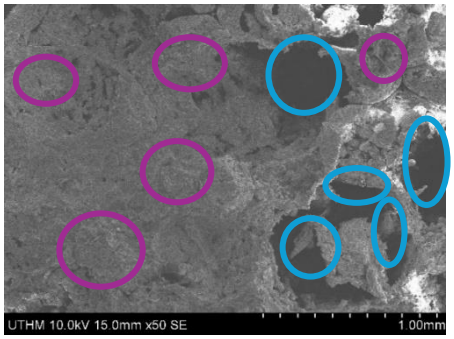	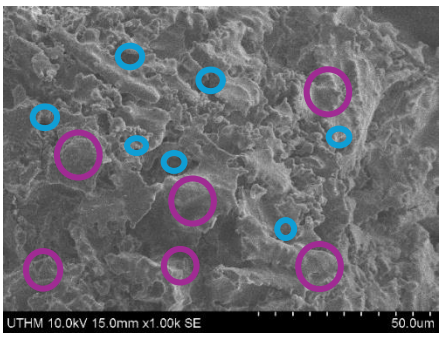

Research Progress in Mechanical and Manufacturing Engineering Vol. 6 No. 2 (2025) p.18-26

C1-2-45

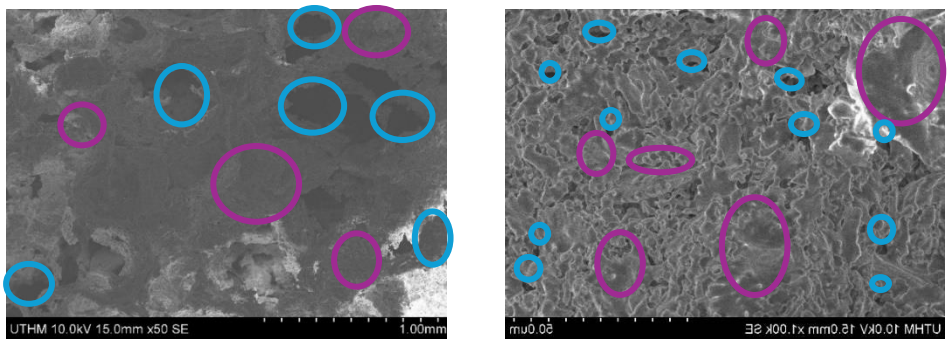

C1-3-45

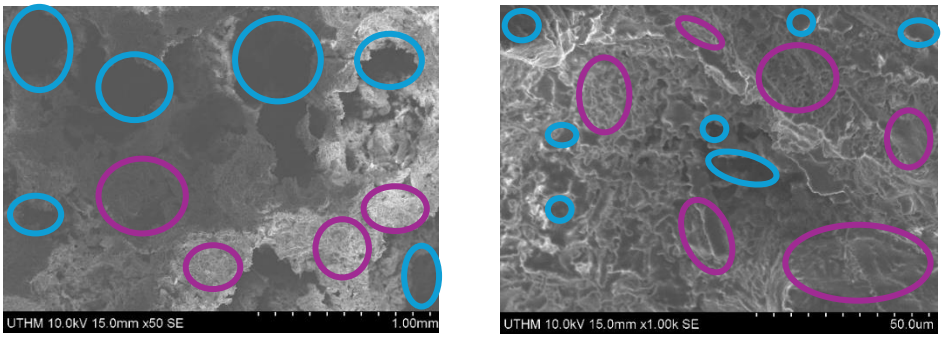

Fig. 2 *Microstructure of silica foam at composition 45wt%*

All samples C2-1-50, C2-2-50, and C2-3-50 were captured under 50x and 1000x magnification to analyze the pore morphology and strut microstructure of silica foam at 50 wt.% silica composition. Samples C2-1-50, C2-2-50, and C2-3-50 each exhibit a dual-phase pore structure comprising open and closed pores with predominantly circular geometry, critical for balancing permeability and mechanical stability [5]. C2-1-50 presents a moderately porous network with randomly distributed pores, where the granular strut morphology indicates effective sintering and contributes to a higher reactive surface area, key for fluid transport and filtration. C2-2-50 features more irregular pore placement and size variations, likely due to localized slurry absorption or thermal gradients during sintering; its well-defined, rough struts enhance both particle capture and interfacial bonding. C2-3-50 maintains a relatively uniform pore distribution, and its finely textured struts imply strong sintering and structural cohesion, making it suitable for long-term filtration performance under mechanical stress.

Sample	50x magnification	1000x magnification
C2-1-50	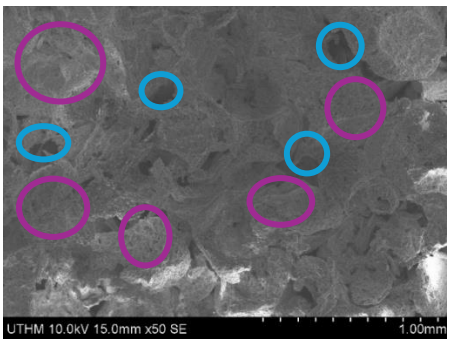	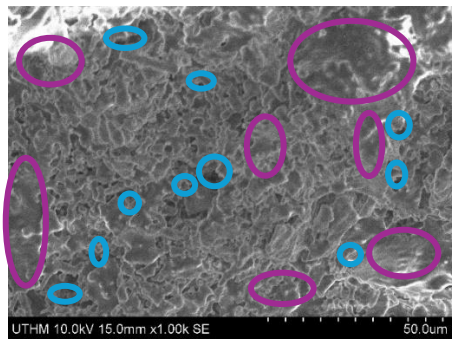

C2-2-50

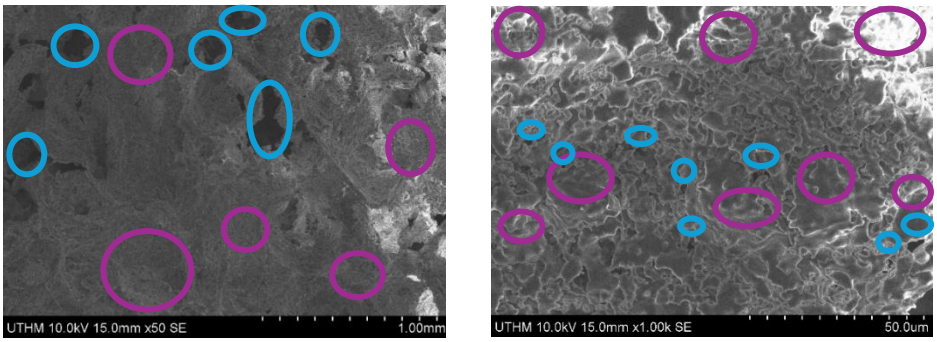

C2-3-50

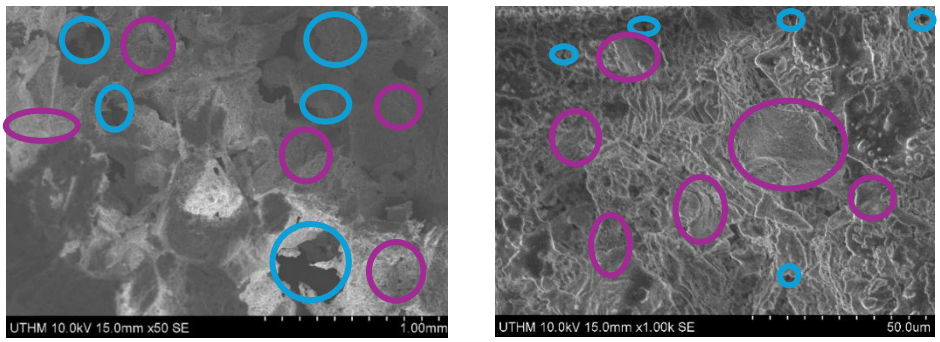

Fig. 3 *Microstructure of silica foam at composition 50wt%*

All Samples C3-1-55, C3-2-55, and C3-3-55 were examined under 50x and 1000x magnification to assess the pore morphology and strut microstructure of silica foam at 55 wt.% silica composition. Samples C3-1-55, C3-2-55, and C3-3-55 display a pore compactness increase, forming a more closed-cell architecture, consistent with densification that reflect high silica loading and reduced porosity [6]. C3-1-55 presents a densely packed microstructure with granular struts, indicating robust sintering and elevated compressive strength at the expense of fluid permeability. C3-2-55 continues this trend with tightly distributed small pores and refined strut textures, suggesting enhanced structural cohesion and durability under operational stress. C3-3-55 exhibits uniform, closely spaced pores and consistently rough strut surfaces, signaling a mechanically stable foam matrix optimized for filtration systems where strength and long-term integrity outweigh high throughout.

Sample	50x magnification	1000x magnification
C3-1-55	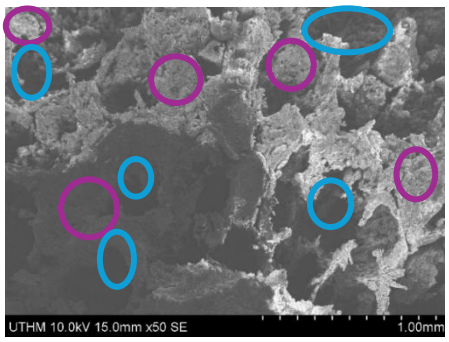	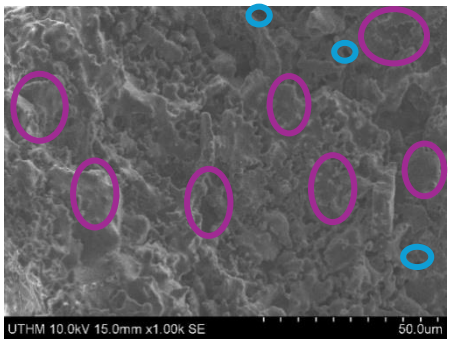

C3-2-55

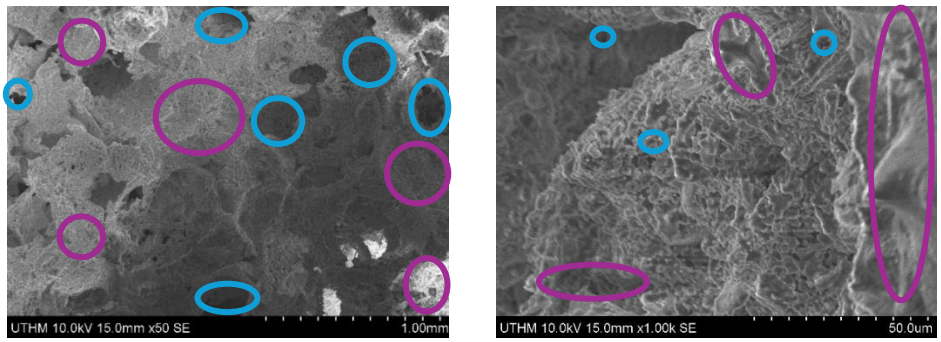

C3-3-55

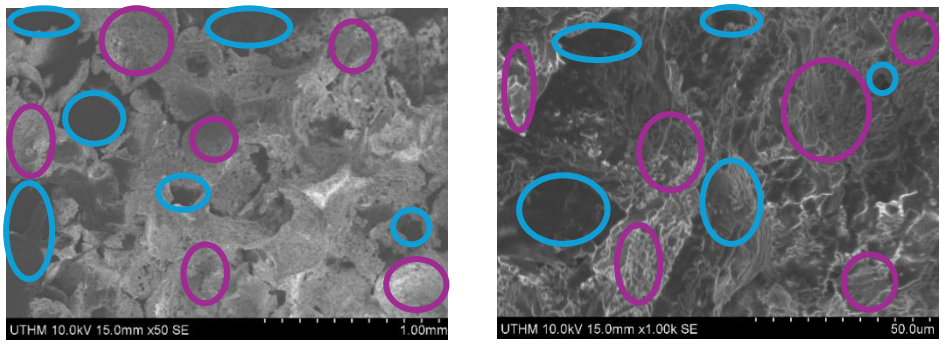

Fig. 4 *Microstructure of silica foam at composition 55wt%*

3.2 Density and Porosity

This analysis focuses on how using PEG and CMC binders affects the density and porosity of SiO_2 foam. As expected from material science principles, higher density results in lower porosity. Our results confirmed this inverse relationship denser foam structures had fewer pores, highlighting the binder's role in shaping the foam's overall morphology and performance. Table 2 and Fig. 5 show the density and porosity of silica foam sintered at 1200°C.

Table 2 *Data collected for density and porosity at 1200° C*

Composition	Sample	Average density (g/cm^3)	Average porosity (%)
45	A1-1-45	0.5807	69.61
	A1-2-45		
	A1-3-45		
50	A2-1-50	0.5591	64.42
	A2-2-50		
	A2-3-50		
55	A3-1-55	0.6115	66.06
	A3-2-55		
	A3-3-55		

The density of silica foam was influenced by the silica content in the slurry at a sintering temperature of 1200°C. The sample with 55 wt.% silica showed the highest density (0.5807 g/cm^3), while the 50 wt.% sample had the lowest (0.5591 g/cm^3), due to its more open pore structure observed via SEM. Increased porosity leads to lower density and better water permeability, which is beneficial for filtration. However, higher silica content results in denser, stronger foam with reduced porosity, potentially limiting filtration efficiency. These findings highlight the need to balance silica content to optimize both mechanical strength and filtration performance. Porosity of the silica foam was influenced by the silica content in the slurry. The sample with 45 wt.% silica

showed the highest porosity (69.61%), while the 50 wt.% sample had the lowest (64.42%). The 55 wt.% sample had moderate porosity (66.06%). Higher silica content led to tighter particle packing during sintering, resulting in reduced porosity and increased structural strength. In contrast, higher porosity improves water flow but may compromise mechanical integrity. Similarly, such microstructural refinement improves mechanical durability in porous bioceramics, further supporting the results obtained here [7]. These results highlight the importance of optimizing silica composition to balance filtration efficiency and mechanical durability.

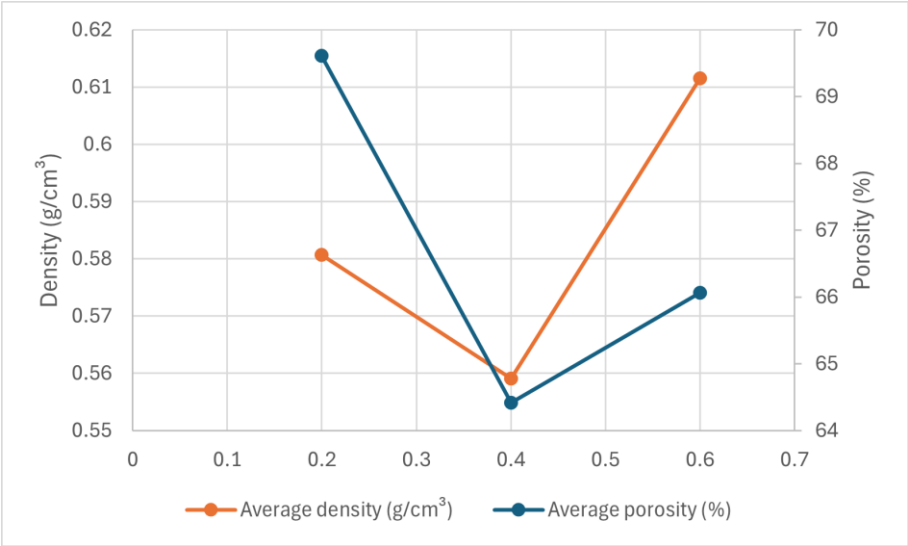

Fig. 5 *Graph of average density and porosity at different compositions*

3.3 Compressive Strength

Compressive strength testing was carried out to assess the mechanical performance of silica foams. The results are summarized in Table 3 and Fig. 6

.

Table 3 *Data collected for compressive strength at 1200° C*

Composition	Sample	Compressive Strength (N/mm²)	Compressive Strength (N/mm²)
45	B1-1-45	0.0787	0.1015
	B1-2-45	0.1546	
	B1-3-45	0.0713	
50	B2-1-50	0.0474	0.0808
	B2-2-50	0.0642	
	B2-3-50	0.1308	
55	B3-1-55	0.1286	0.162
	B3-2-55	0.1798	
	B3-3-55	0.1776	

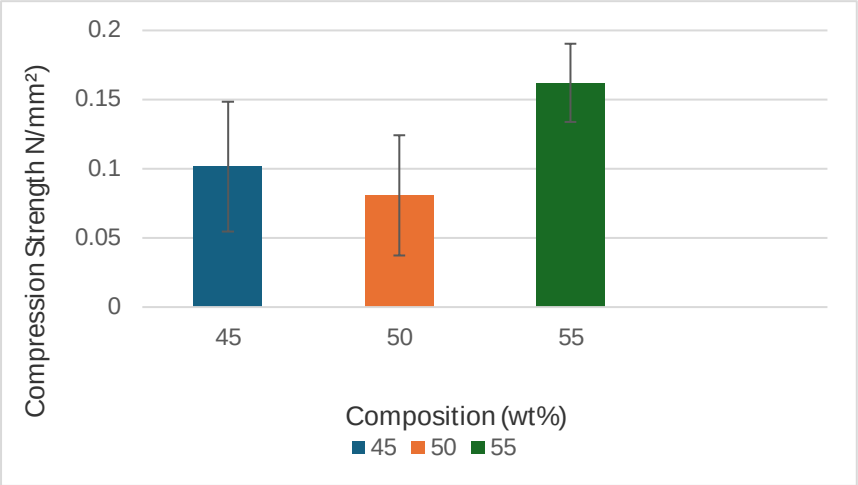

Fig. 6 *Graph of average porosity at different compositions*

Compressive strength of the silica foam increased with higher silica content. The 55 wt.% sample showed the highest strength due to its lower porosity and denser microstructure, making it ideal for filtration applications requiring structural durability. In contrast, the 50 wt.% sample had the lowest strength, attributed to its higher porosity and weaker structure, as confirmed by SEM analysis. These results emphasize the importance of optimizing silica composition to balance mechanical performance and filtration efficiency. Similarly, it has been found that the binder type and amount affect pore bonding and strength [8].

4. Conclusion

This study demonstrated that silica composition significantly affects the structural and mechanical performance of ceramic water filters produced via the foam replication method. Among the tested formulations, the 55 wt.% silica sample showed the best balance of density, porosity, and compressive strength, making it the most suitable for filtration applications. A higher silica content improved particle packing and reduced defects, whereas excessive porosity in lower silica samples compromised mechanical integrity [9]. These findings highlight the importance of optimizing silica content to achieve both durability and filtration efficiency.

Acknowledgement

The authors would like to thank the Faculty of Mechanical and Manufacturing Engineering at Tun Hussein Onn Malaysia for its support in completing their research work.

Conflict of Interest

The authors declare that they have no conflict of interest regarding the publication of this paper.

Author Contribution

The authors confirm sole responsibility for the following: study conception and design, data collection, analysis and interpretation of results, and manuscript preparation.

References

[1] Bush, J. A., Vanneste, J., Gustafson, E. M., Waechter, C. A., Jassby, D., Turchi, C. S., & Cath, T. Y. (2018). Prevention and management of silica scaling in membrane distillation using pH adjustment. *Journal of Membrane Science*, 554, 366–377. https://doi.org/10.1016/j.memsci.2018.02.059

[2] Angenoorth, J., Erhard, P., Wächter, D., Volk, W., & Günther, D. (2024). Sintering of 3D-printed aluminum specimens from the slurry-based binder jetting process. *Progress in Additive Manufacturing*, 9(3), 633 642. https://doi.org/10.1007/s40964-024-00657-2

[3] Ahmad, S., Latif, M. A., Taib, H., & Ismail, A. F. (2013). Short Review: Ceramic Foam Fabrication Techniques for Wastewater Treatment Application. *Advanced Materials Research*, 795, 5–8. https://doi.org/10.4028/www.scientific.net/amr.795.5

[4] Bansode, S.N., Phalle, V.M. & Mantha, S.S. (2020). Influence of Slurry Composition on Mould Properties and Shrinkage of Investment Casting. *Trans Indian Inst Met* 73, 763–773. https://doi.org/10.1007/s12666-020-01872-5
[5] Baharom, S., Ahmad, S., Taib, H., & Muda, R. (2016). The effects of composition and sintering temperature on the silica foam fabricated by slurry method. *AIP Conference Proceedings*, 1756, 020004. https://doi.org/10.1063/1.4958747
[6] A. Krüger, M. Lisker, (2019). Comparison of fumed Silica- and colloidal Silica Slurry for CMP. Research Gate. https://www.researchgate.net/publication/338038555_Comparison_of_fumed_Silica-and_colloidal_Silica_Slurry_for_CMP
[7] Baino, F.; Caddeo, S.; Novajra, G.; Vitale-Brovarone, C. (2016). Using porous bioceramic scaffolds to model healthy and osteoporotic bone. *Journal of European Ceramic Society*, 36, 2175–2182.
[8] A.Kristoffersson, E.Roncari and C. Galassi, (1999). "Comparison of different binders for water-based tape casting of alumina. *Doktorsavhandlingar Vid Chalmers Tekniska Hogskola*, 2219(1525), 2123-2131
[9] Accorsi, J., Yu, M. (1998). Carbon black. In: Pritchard, G. (eds) Plastics Additives. *Polymer Science and Technology Series*, 1, https://doi.org/10.1007/978-94-011-5862-6_18